NASA-185
Univ. Corp. for Atmospheric Research

NCAR Manuscript No. 68-140

STRUCTURAL MEASUREMENTS ON BALLOONS IN FLIGHT

by

Karl H. Stefan
Scientific Balloon Facility

GPO PRICE $ _____
CFSTI PRICE(S) $ _____
Hard copy (HC) _____
Microfiche (MF) _____
ff 653 July 65

July 1968

NATIONAL CENTER FOR ATMOSPHERIC RESEARCH
Boulder, Colorado

N68-37280
(ACCESSION NUMBER) (THR
27
(PAGES) (CODE)
CR-97268
(NASA CR OR TMX OR AD NUMBER) (CATEGOR
FACILITY FORM 602

OCT 1968
RECEIVED
NASA STI FACILITY
INPUT BRANCH

ABSTRACT

NCAR has developed an instrumentation system designed to collect data, during a balloon ascent, on balloon environment, shape, film strain, and film temperature. The total system is described, as are the sensors and techniques for using them. Limited data collected from three flights indicate that the system will provide a powerful tool for diagnosis of balloon problems.

STRUCTURAL MEASUREMENTS ON BALLOONS IN FLIGHT

The Scientific Ballooning Facility at NCAR has begun a basic, long range program, involving coordinated analytical and experimental approaches, to predict stresses in balloons during ascent. We are developing instrumentation for measuring as many balloon structural parameters as possible and, by means of a series of balloon flights, we are determining and studying the important parameters. At this point we are primarily interested in the balloon during ascent.

BALLOON SYSTEM

The experimental program employs a system consisting of two balloons in a tandem arrangement, connected by a "tow" line. The upper balloon, tethered to the top end fitting of the main balloon by a 200 ft line, carries two downward-looking cameras to photograph the top of the main balloon. The upper balloon also carries a large parachute for lowering the main balloon and/or the camera package. Bolted to the top end fitting of the main balloon is a 25 lb package, containing three-axis accelerometers, a differential pressure sensor, telemetry equipment, and power supply. A ground plane antenna (about 1 ft diam) hangs inside the balloon about 20 ft from this package. Film strain and temperature gauges are mounted at selected locations on the upper part of the balloon and are connected to the telemetry package by wire leads. The main gondola carries normal balloon instrumentation and upward-looking cameras mounted on the ends of 25 ft booms. Figure 1 shows the experimental configuration in the air.

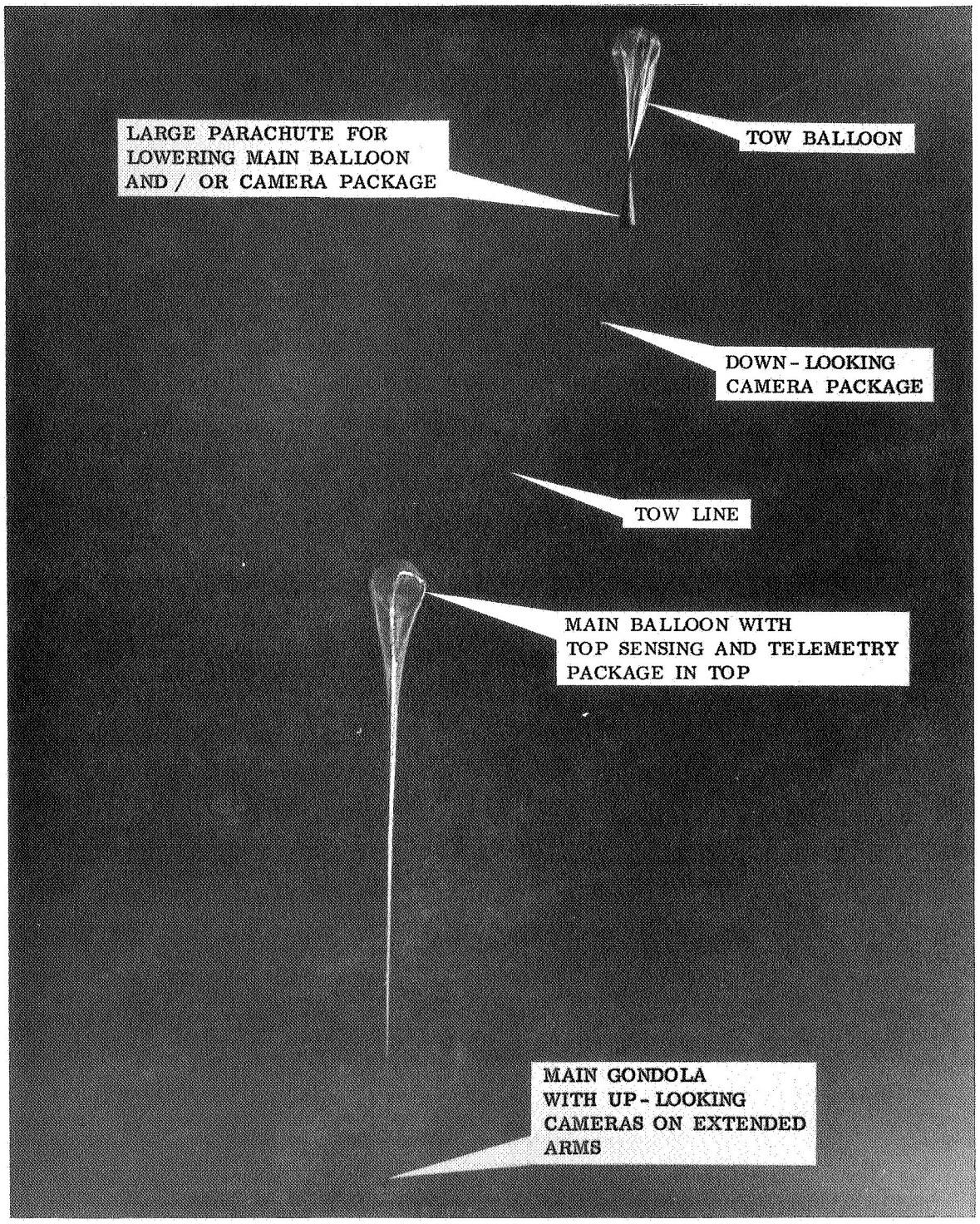

Fig. 1 NCAR two-balloon system

Naturally, we insure that the upper balloon will tend to have a greater ascent rate than the main balloon. This practice has worked out quite well, with the top balloon oscillating from side to side, taking pictures of the main balloon from all angles. (The upper balloon camera arrangement was originated by Thomas Bilhorn at NCAR several years ago.) When float altitude for the top balloon is approached, the tether line is squibbed off at the top end fitting and the balloons separate. In the case of main balloon failure before float altitude is reached, the upper parachute opens when descent commences, the upper balloon is released, and the entire lower system, including the main balloon, descends on the parachute. The parachute is rigged with a central load line so that the canopy is slack and free for opening at small descent rates.

Three flights in the past year have used this system: a Viron 2.94 MCF balloon which burst at 45,000 ft (NCAR Flight 321); a Raven 9.0 MCF cone-top balloon (NCAR Flight 338); and a conventional Raven 3.5 MCF balloon (NCAR Flight 621).

PHOTOGRAPHY SYSTEM

A 16 mm Bell & Howell Model 70 camera is mounted on each end of the long-armed gondola shown in Fig. 2. Four-hundred ft magazines enable a 1/sec frame rate for a normal ascent period. Figure 3 is a frame taken with the upward-looking cameras, showing the top balloon in position above the main balloon. The top balloon oscillates, allowing the downward-looking camera to photograph the main balloon from various angles. Using Kodachrome II film, a setting of f/22 at 1/14 sec gave good exposures. The long boom mounting gives an unencumbered view of the balloon train.

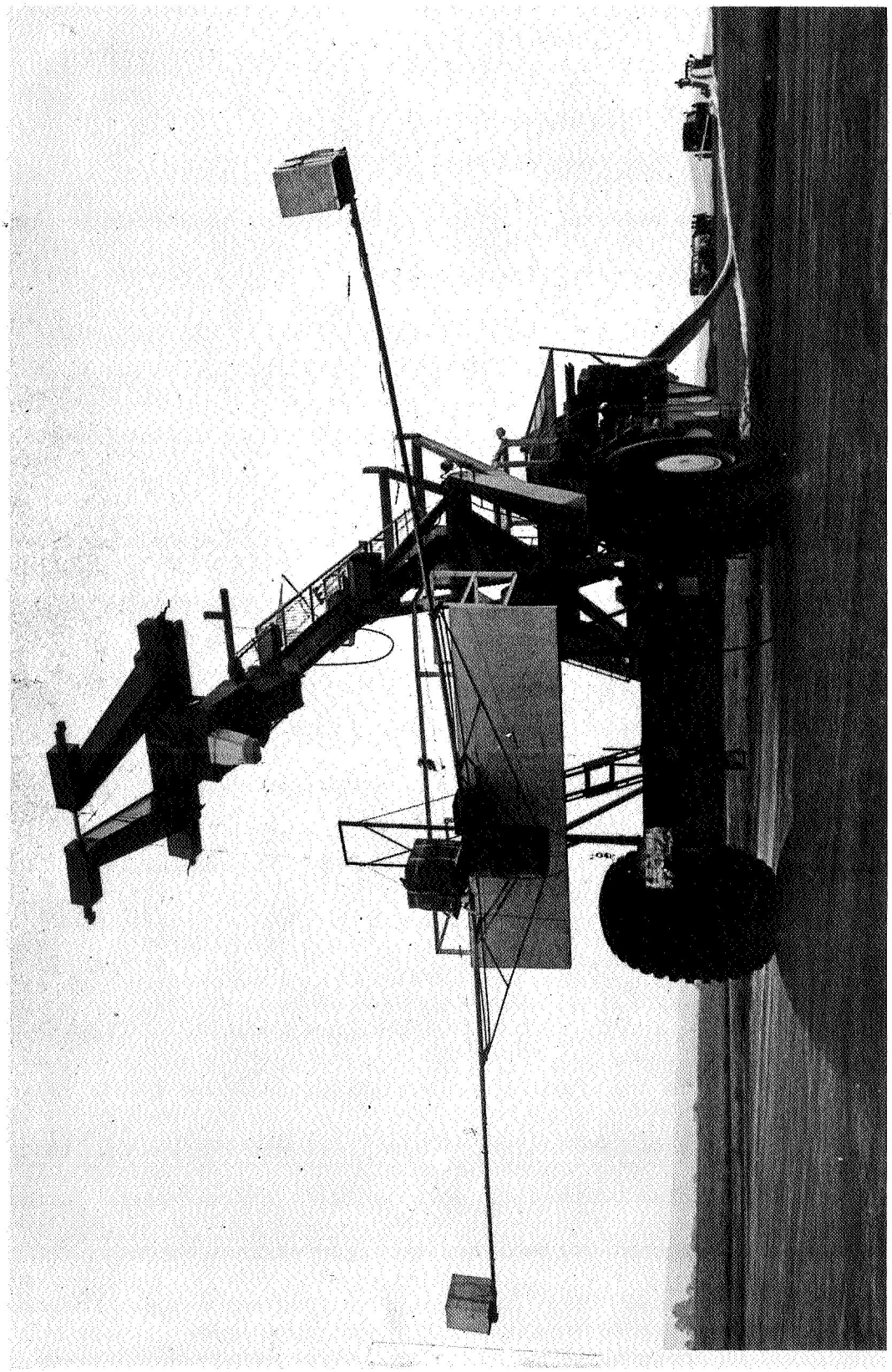

Fig. 2 Cameras mounted on gondola

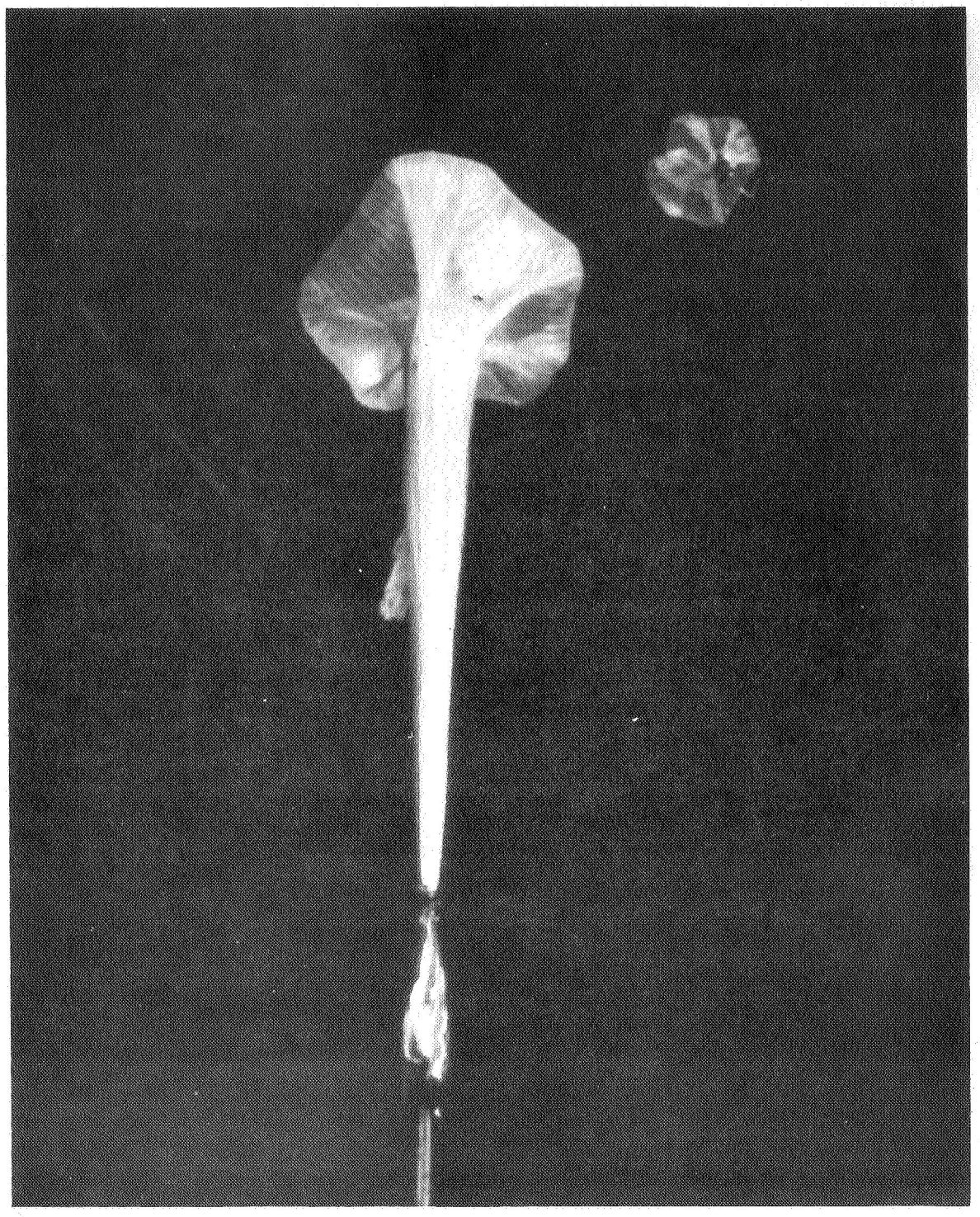

Fig. 3 Two-balloon system, showing top balloon in position above main balloon

These pictures have enabled us to record the balloon shape during ascent, and have shown perturbations such as relative wind gusts and shear winds, which often flutter the loose material, occasionally forming a sail. The greatest perturbations during this series were observed during penetration of a 150 kt jet stream. These perturbations caused two or three spinnakers to form, each of which lasted for a few seconds. Movies taken with the upward-looking camera have recorded one or two occasions on which the material in the balloon is suddenly rearranged, sometimes in less than a second.

Figure 4 shows the upper camera package, which in flight is suspended beneath the upper balloon and looks down at the main balloon. We have used two cameras, a 16 mm Bell & Howell Model 70 and a Northridge 35 mm pulsed camera, both with 400 ft magazines. Our best resolution pictures have been obtained with the Northridge camera, using medium speed Ektachrome at f/5.6 and 1/360 sec.

Figures 5 to 8 are photographs of a Viron 2.94 MCF balloon over NCAR's Palestine balloon base. Figure 5 shows the balloon at 10,000 ft, with a red plastic streamer on the tow line, which helped to indicate winds during ascent. The balloon at this altitude has a single cleft, typical of balloons that are not fully tailored. Figure 6 shows the same balloon at 46,000 ft, just before balloon failure. By observing this and other slides at different angles, we can see what appears to be a band of circumferential stress around the balloon.

Figure 7 shows holes that have developed in the balloon in the 1 sec since the previous slide was taken. The stressed band has disappeared,

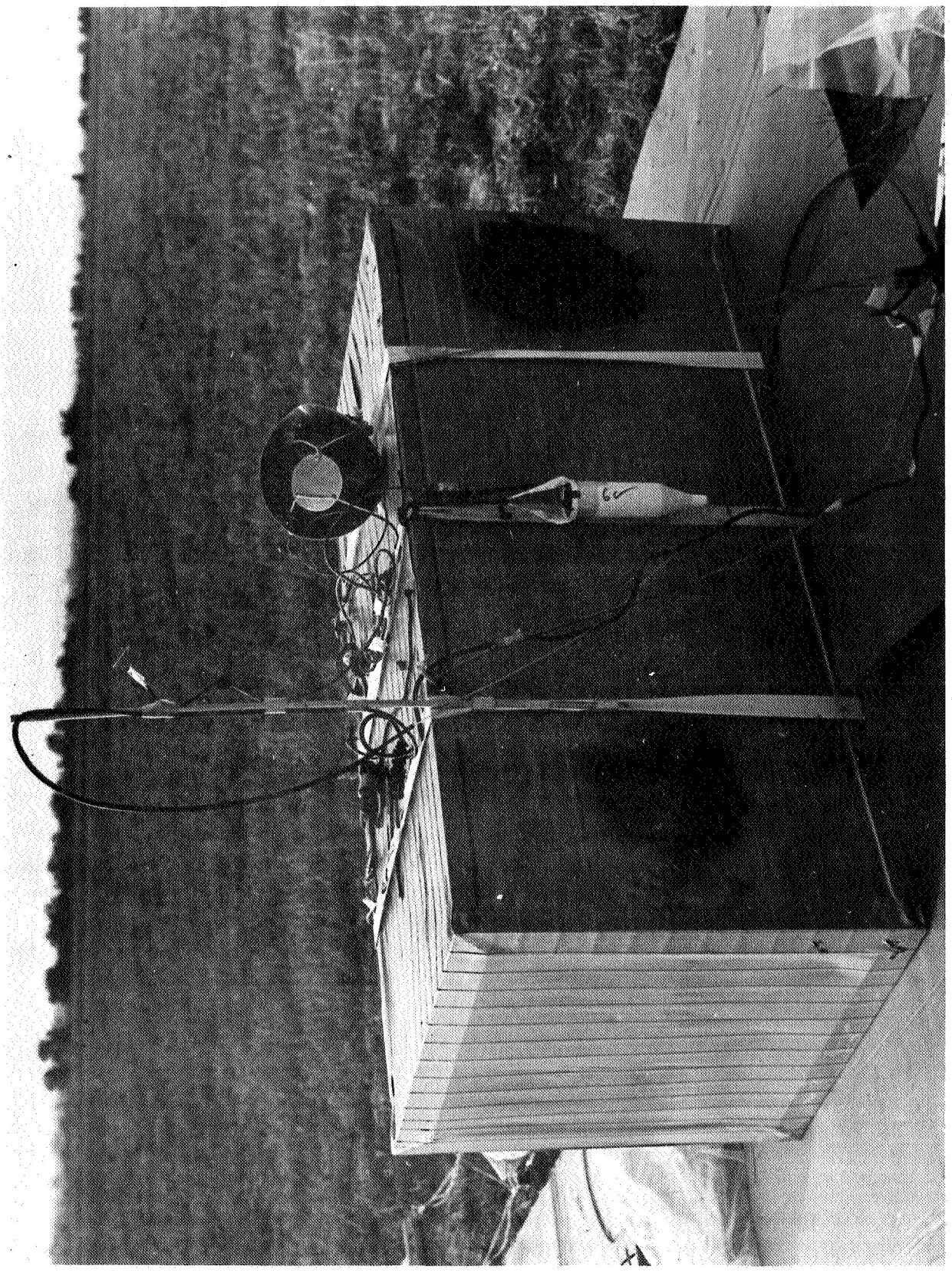

Fig. 4 Upper camera package

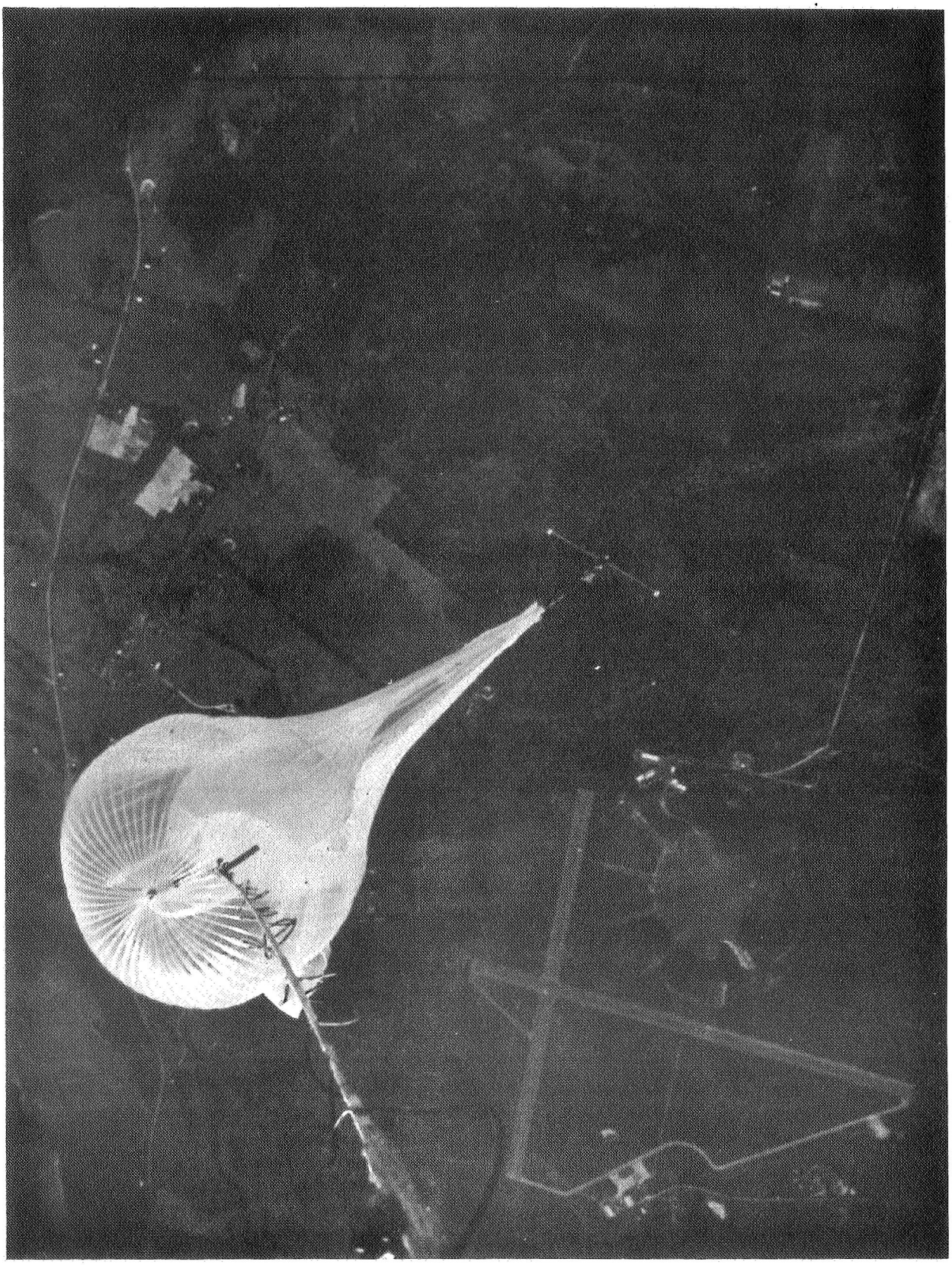

Fig. 5 Viron 2.94 MGF balloon at 10,000 ft

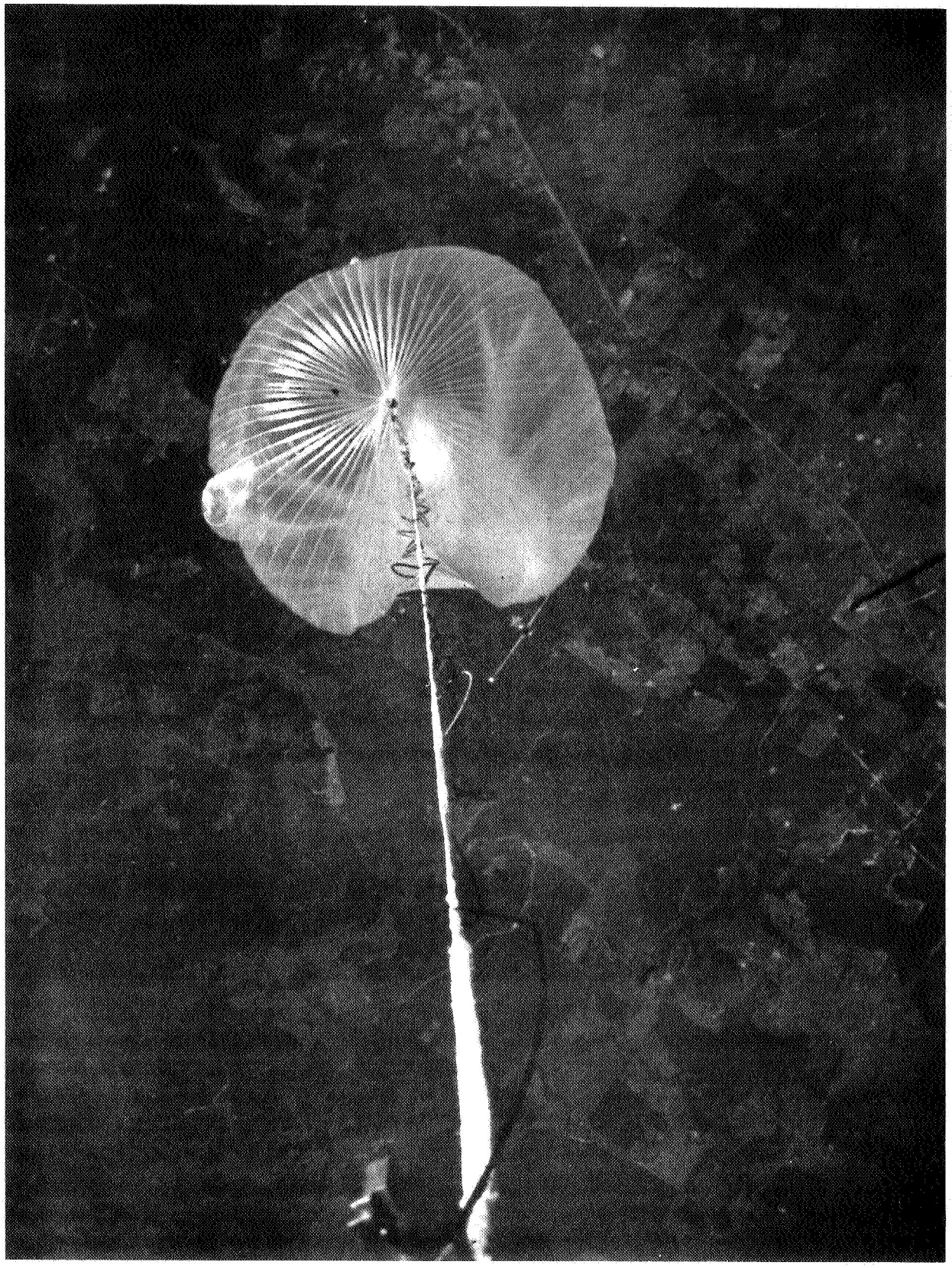

Fig. 6 Viron balloon at 46,000 ft, showing circumferential stress band

Fig. 7 Viron balloon at 46,000 ft, with holes in balloon film

Fig. 8 Viron balloon at destruction stage

apparently relieved by the holes in the balloon. In Fig. 8, taken 1 sec later, destruction of the balloon is complete.

A 9.0 MCF experimental balloon built by Raven is shown in Figs. 9 to 11. Figure 9 shows the reinforced Mylar conical top, which at this stage of inflation gives a smooth, symmetrical shape to the top of the balloon, in contrast to the Viron balloon with its large cleft and roll of material extending into the top end fitting. We are not yet certain of the significance of this top configuration, but it does permit stress predictions for this portion of the flight because of its symmetry.

Figure 10 shows the same 9.0 MCF balloon at 68,000 ft. Here the conical cap, having become fully inflated at about 55,000 ft, is quite apparent. Another view of the same balloon at 69,000 ft (just prior to release of the upper balloon) is shown from a different angle in Fig. 11.

FILM STRAIN MEASUREMENTS

We are still in the learning process with regard to measuring film strain, but measurements to date made with our film strain sensor, shown in Fig. 12, have proved partially successful.

The film strain gauge is normally mounted in the middle of a gore. A Mylar strip is masked in a sawtooth pattern and passes through a slot in the head which carries a light source and a photoelectric cell. The end of the tape and the photocell are anchored to the balloon film 2 in. apart, and as the film over this 2 in. span elongates, the tape is pulled through the cell, and the sawtooth masking causes a variation in the photocell output. The power leads and signals run through fine wires to an amplifier

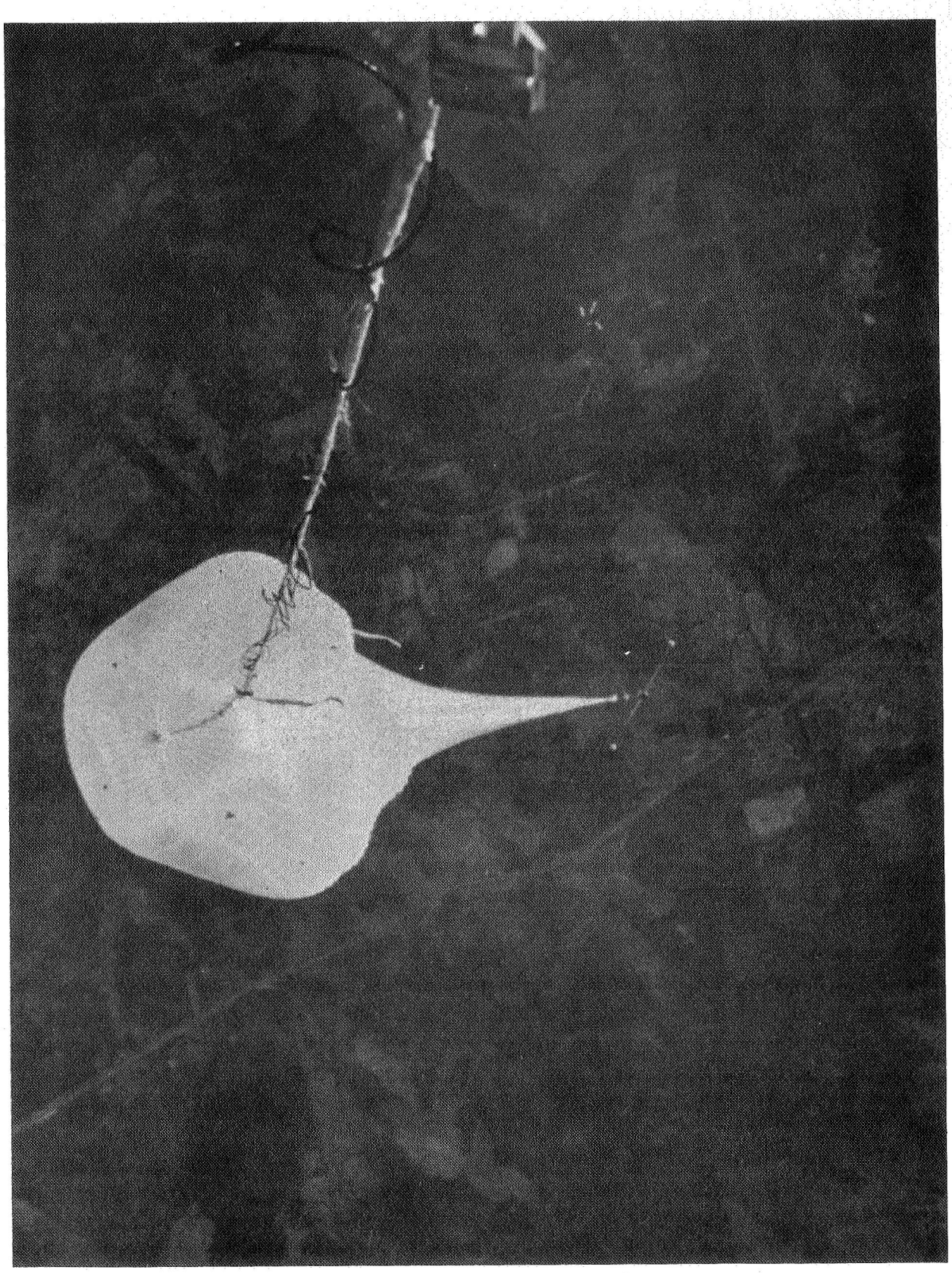

Fig. 9 Raven 9.0 MCF experimental balloon

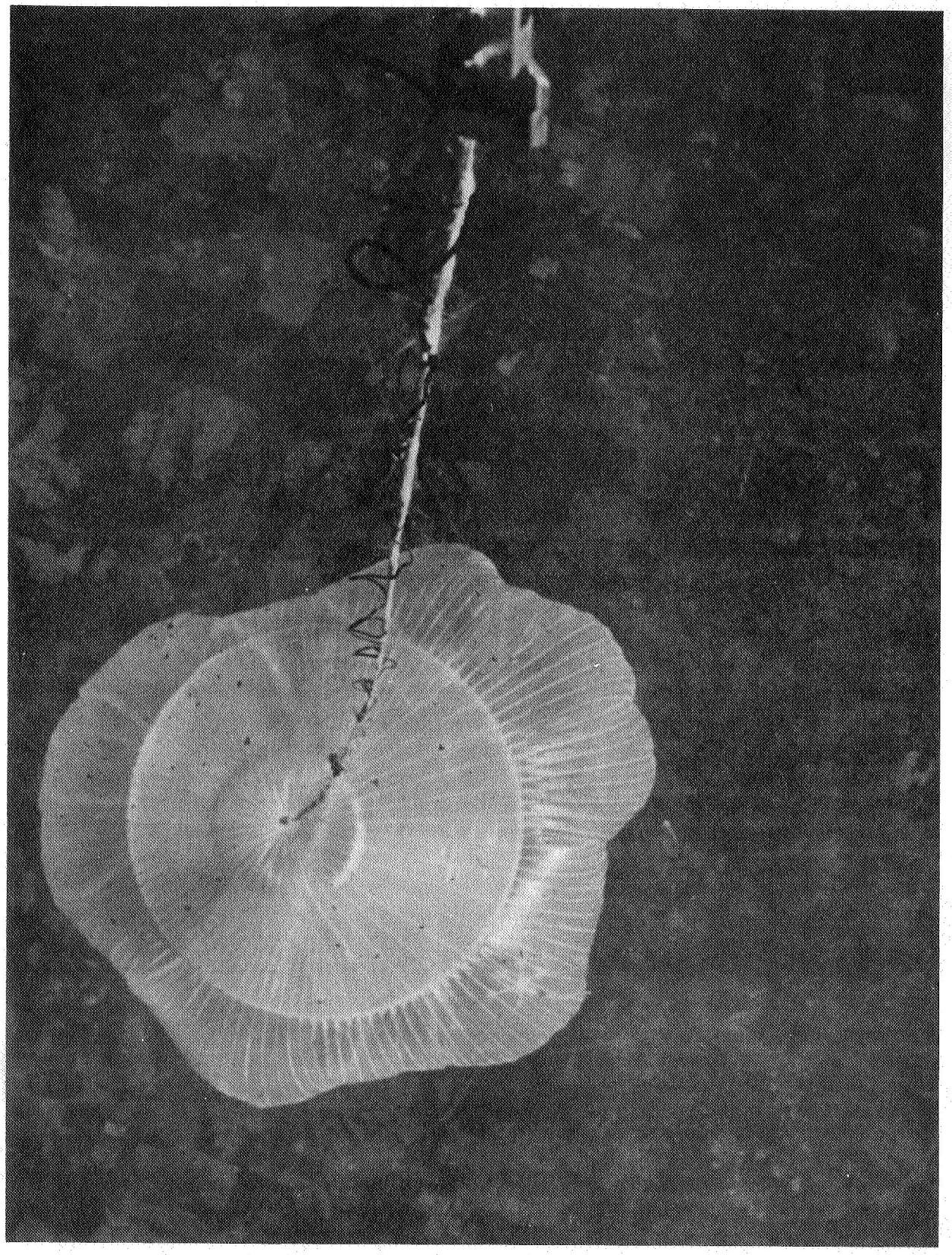

Fig. 10 Raven balloon at 68,000 ft, showing fully inflated conical top

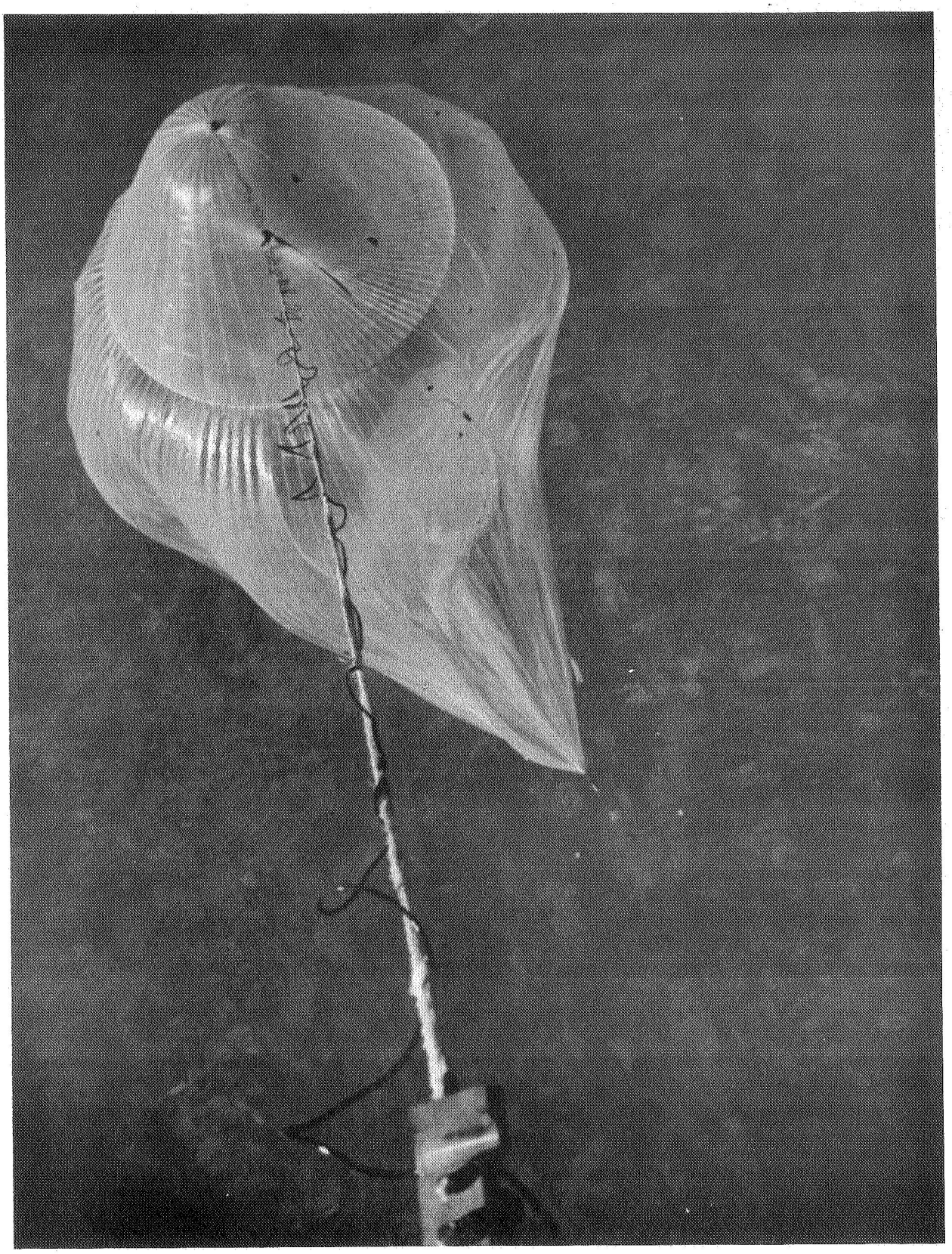

Fig. 11 Raven balloon at 69,000 ft

fastened to the load tape, and the amplified signal (0-5 V) is carried up the load tape to the telemetry package. Figure 13 shows a strain gauge mounted on balloon film ready for flight.

We have obtained excellent results with this film strain sensor under controlled conditions, such as test inflations in a sheltered area. However, because the sensor is troublesome in field operations -- the lights burn out, output is extremely voltage-sensitive and power consumption is fairly high -- we are trying to develop a more reliable device. We are now developing a strain sensor using the same sliding principle, but having a variable reluctance tape which hopefully will eliminate our present troubles without introducing new ones.

Figure 14 shows an example of an ascent strain measurement, from launch to 20,000 ft. The gauge was located 26 ft from the top of the balloon -- 8 ft above the stressed band shown in Fig. 6. The measurement shows some circumferential strain in the balloon material, indicating circumferential stress in this conventional balloon design during ascent. We hope that future measurements will give us a complete picture of stress distributions during ascent for a variety of balloon designs.

FILM TEMPERATURE MEASUREMENTS

Film strain can be better interpreted as stress if the corresponding film temperature history is also known. Therefore, we are determining suitable means to measure film temperature. A small bead thermistor would be the most practical for field use if it could be shown to measure film temperature accurately.

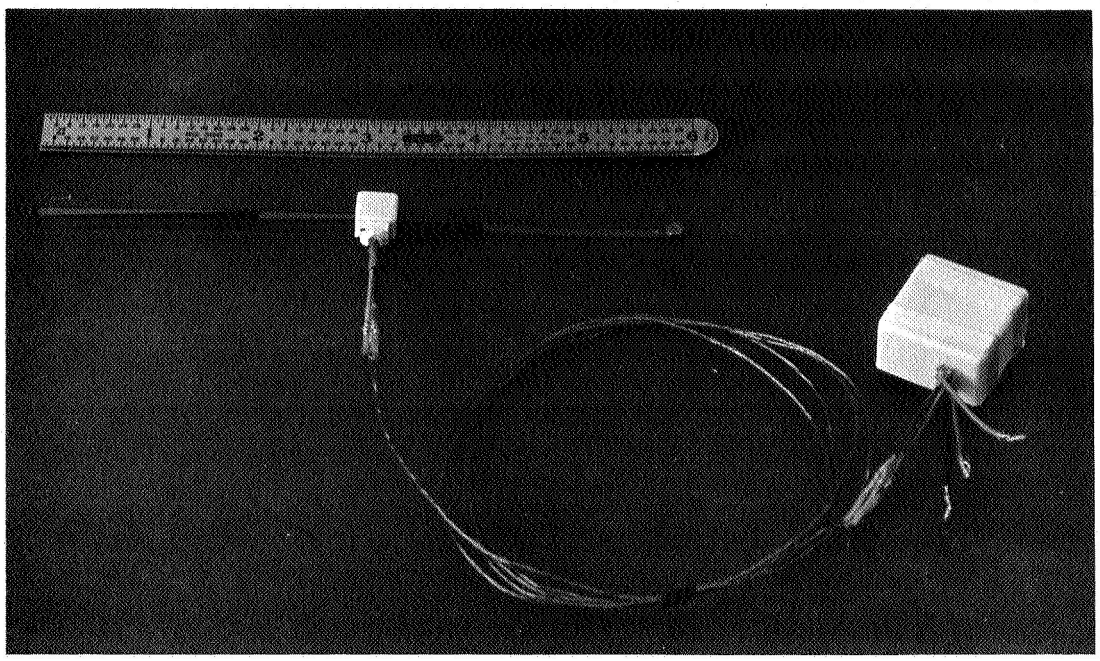

Fig. 12 Film strain sensor

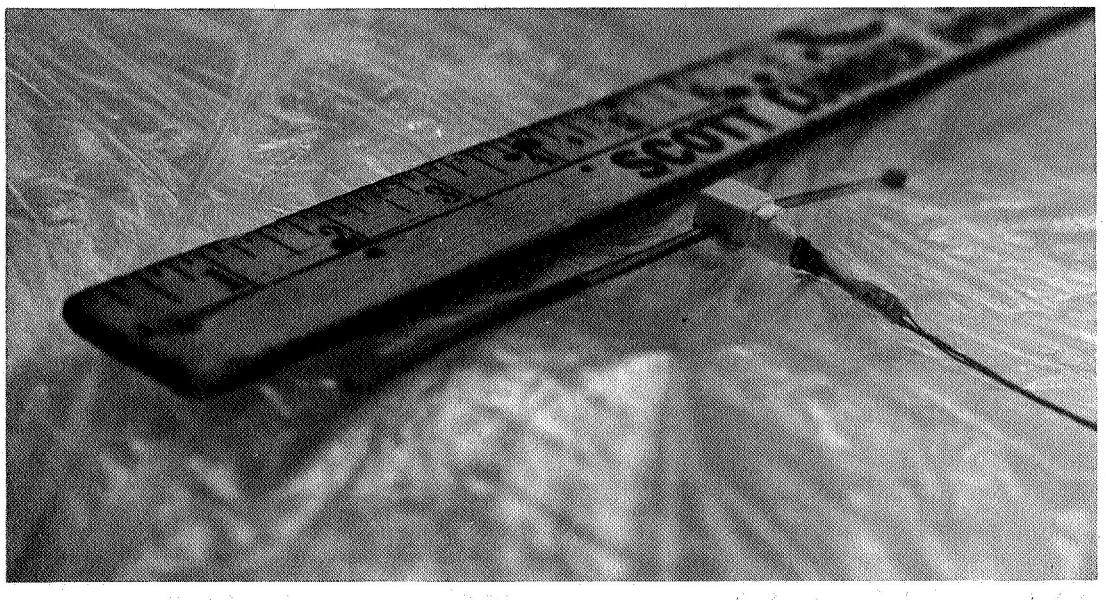

Fig. 13 Mounted film strain gauge

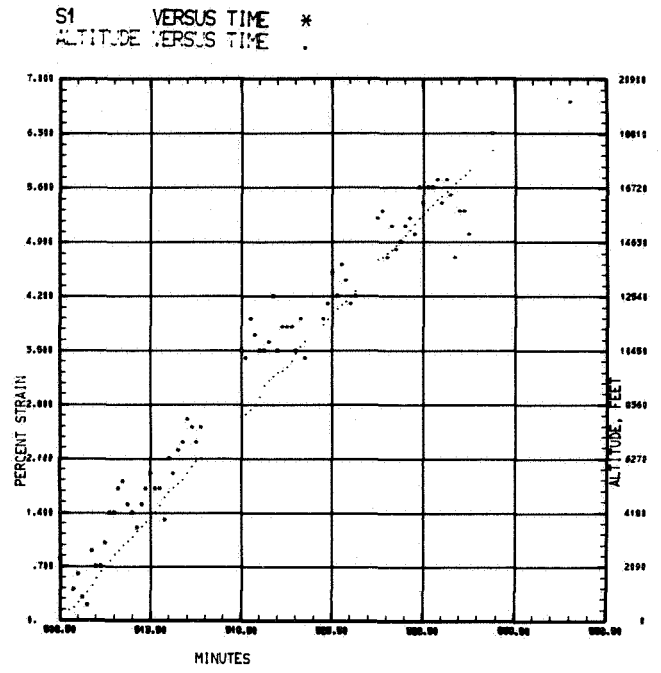

Fig. 14 Ascent strain measurement

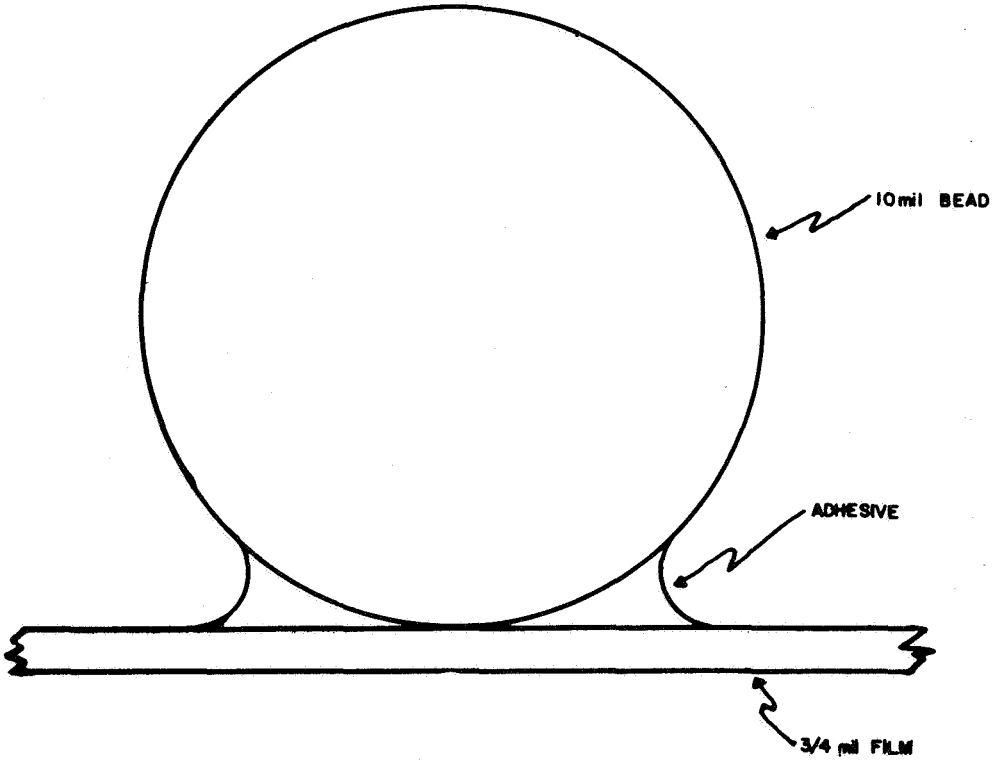

Fig. 15 Thermistor mounted on balloon film

Figure 15 compares the size of a 10 mil bead thermistor to the thickness of the 0.75 mil film whose temperature it should measure. With a small object, convective heat transfer tends to overpower radiation effects; a 10 mil aluminized bead thermistor, for instance, can measure air temperature quite accurately at pressures as low as 10 mb (*Ney, Maas, and Huch,* 1961). One might surmise, then, that a small thermistor can measure air temperature in the thermal boundary layer next to the balloon skin and, if the boundary layer is thick enough, the measured temperature might approximate that of the skin. In addition, one might expect the thermistor temperature to be slightly biased towards the film temperature by direct conduction into it through the adhesive used to secure the thermistor.

A portion of a thermal boundary layer under a laminar flow condition with a free convection length of about 3 in. is shown in Fig. 16. Here the boundary layer is quite thick compared with 5 and 10 mil bead thermistors. Therefore, if these thermistors do measure the temperature of the air in which they are submerged, the temperature they measure will closely approximate the film temperature. To check this hypothesis further, we buried a fine platinum wire in polyethylene film, mounted various thermistor configurations around it, and measured thermal responses in a bell jar at 10 mb. Figure 17 shows the results. The platinum wire senses the film temperature with an accuracy of $\pm 1^{\circ}C$, and it can be seen that thermistors mounted on the film are approximately at film temperature. The thermistors which are glued on appear to measure more accurately than those which are mounted with a tape overlay. The thickness of the boundary layer appears to be slightly more than an inch under this vertical, natural convection laminar flow condition.

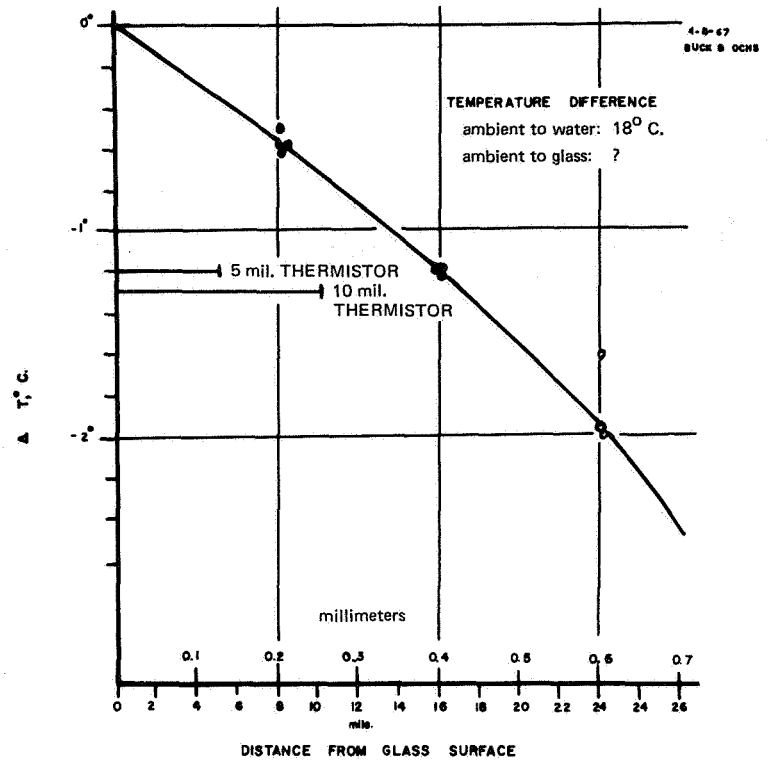

Fig. 16 Experimental measurements of boundary layer temperatures

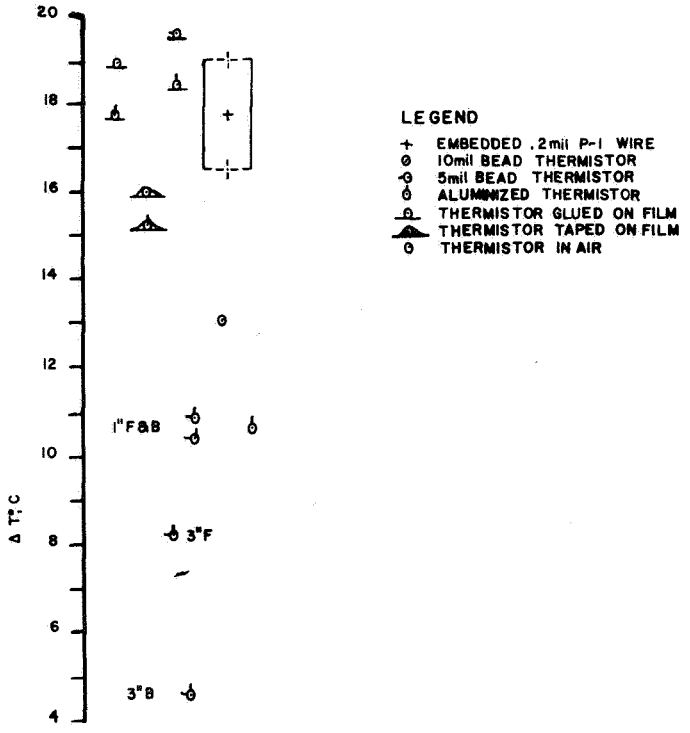

Fig. 17 Film sensor temperature, 30 sec after exposure to 400 BTU/hr radiant heat flux in bell jar, 10 mb pressure

Experiments in the field show that available glues simply have not the strength to hold the thermistors to the film under conditions of folding and rubbing. Therefore, we are presently using the taped-on thermistors, which give measured temperatures slightly lower than the actual temperatures. Aluminum coating makes only a small temperature difference to film-mounted thermistors, even though it makes considerable difference in free air.

Figure 18 shows a thermistor mounted on a balloon wall and ready for flight. The thermistor modulates a 20 mV signal to the top telemetry package. Figure 19 is a plot of temperature vs time (altitude) during ascent. This record is from a 10 mil, uncoated thermistor glued to 0.75 mil polyethylene film about 30 ft from the top of the balloon. The measured temperature approximates ambient temperature, although we did not have an accurate ambient temperature measurement for this flight.

Temperature oscillations increase as altitude increases. One would expect these temperature fluctuations to be linked to balloon rotation, with the sunny side of the balloon always being the warmer. However, balloon rotation data show that even though the rotation period agrees in general with the fluctuation periods, hot and cold peaks do not correlate with the orientation of the thermistor with respect to the sun.

Figure 20 compares glued and overlay mountings of two thermistors mounted immediately adjacent to each other on the same balloon. This composite record shows a temperature difference commencing at about 50,000 ft and increasing to an approximate 6 degree difference at 130,000 ft, with the overlay mounting being the cooler. The glued-on thermistor probably

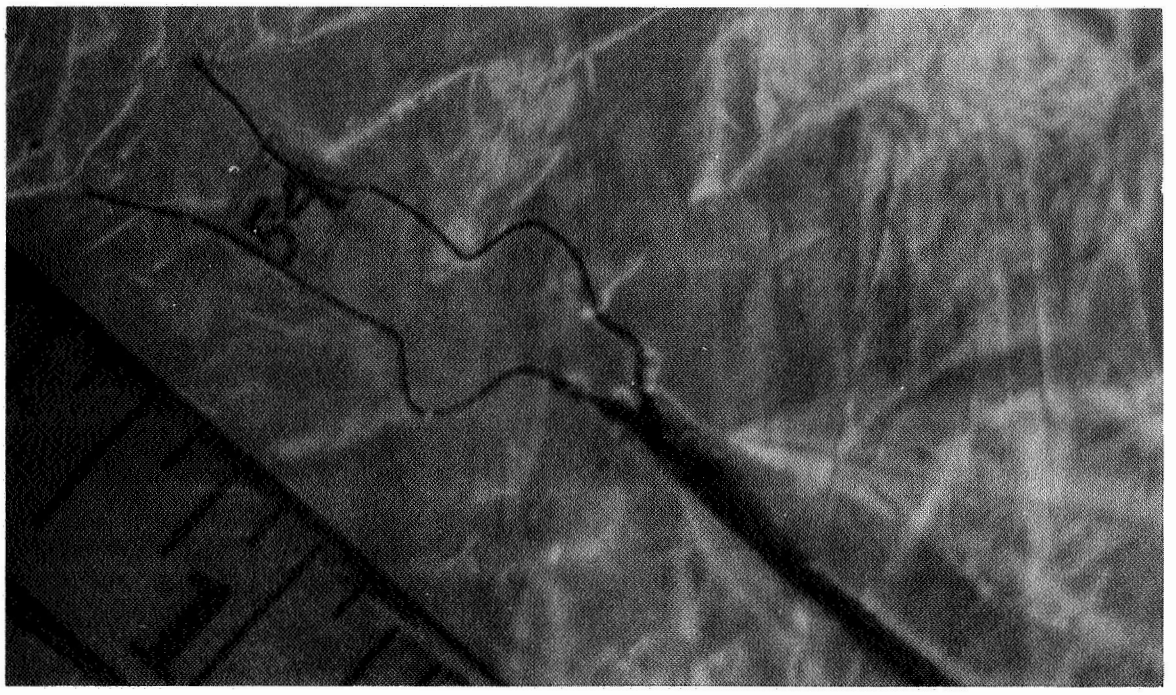

Fig. 18 Thermistor mounted on balloon skin

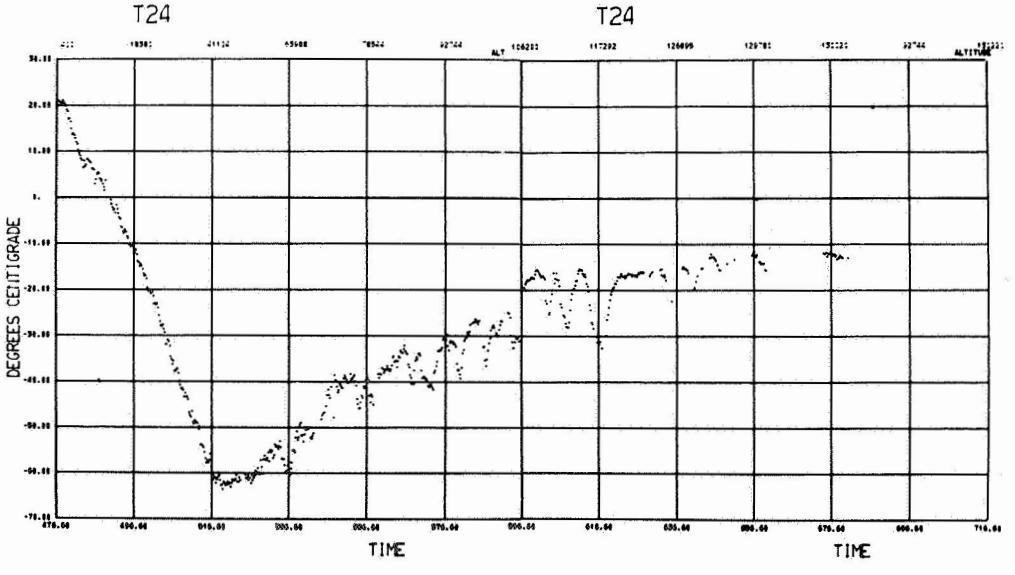

Fig. 19 Measurement of temperature vs time during balloon ascent

more accurately represents film temperature. It remains to be seen whether the temperature error will be consistent enough to permit using the overlay installation.

Figure 21 is a scatterplot curve of measured gas pressures during a balloon ascent; the solid curve is theoretical gas pressure. About half the difference between the curves can be attributed to dynamic pressure due to the rate of ascent of the balloon, while the rest is due to differences of pressure head between theoretical and actual balloons, or to experimental error. The measured pressure trend follows the theoretical, with variations so small as to be insignificant with respect to structural integrity. We can conclude from the pressure record of this particular flight that no significant pressure variations occurred, either from atmospheric perturbations or from blocking of balloon material.

The three-axis accelerometers carried in the top package had a readout system capable of resolving about 0.02 g. While the upper balloon is attached, some slight tugging on the top end fitting of the main balloon was observed; at times, the end fitting was tilted by the pull of the top balloon. Without the attached upper balloon, the top end fitting was very steady. One flight without the upper balloon penetrated a 150 kt jet stream and, though some sailing of the balloon was observed by the upward-looking cameras, top end fitting accelerations of only 0.05 g were observed for one period of about three minutes.

We would like to have accurate relative wind measurements at the top of the balloon, but we have not yet had time to pursue this phase of the program to completion. Mechanical anemometers are the only off-the-shelf devices that could be readily adapted for this purpose, and even

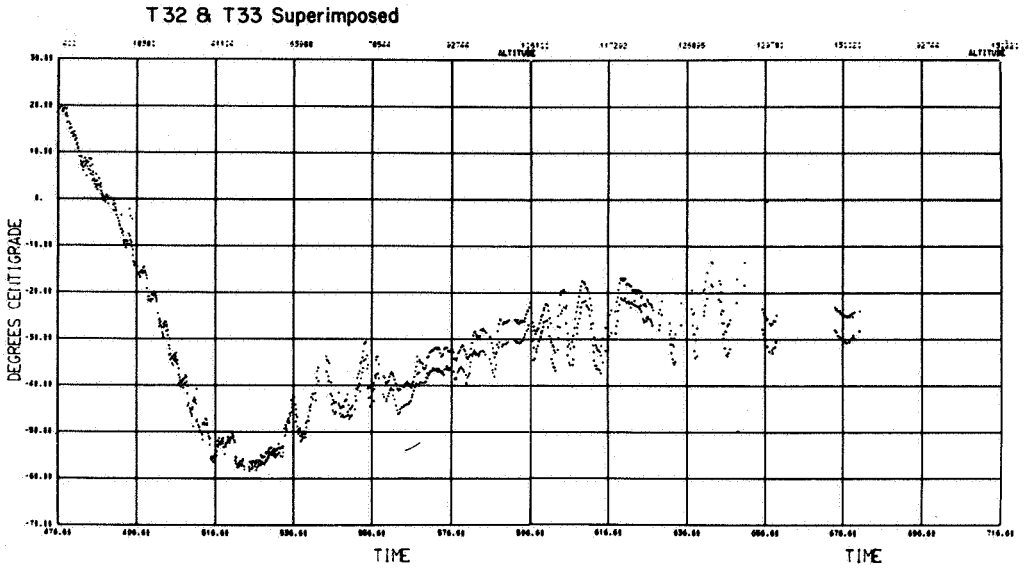

Fig. 20 Composite temperature record, glued and tape-mounted thermistors

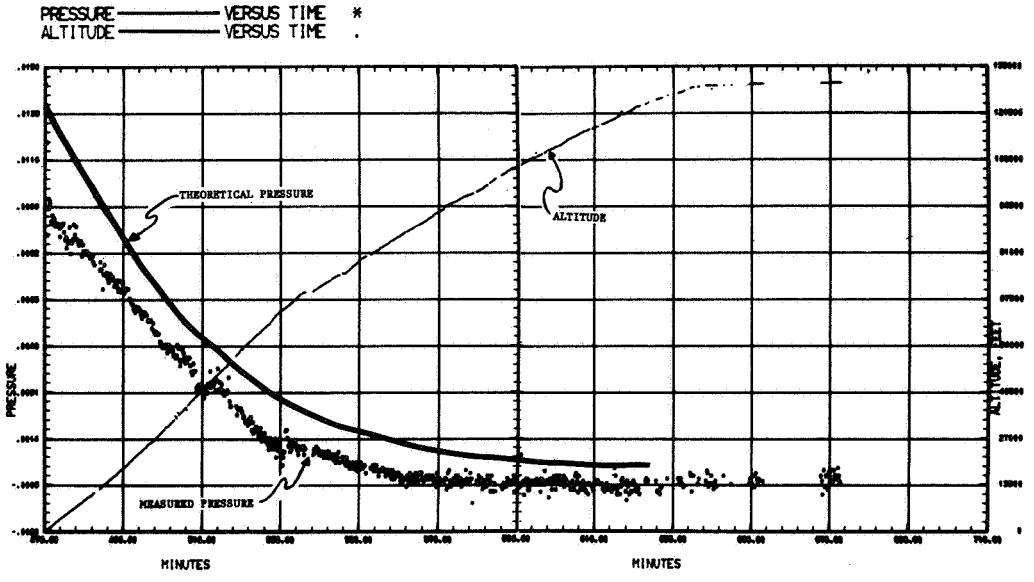

Fig. 21 Measured and theoretical gas pressures during ascent

with the best of these, bearing friction and response times will likely present problems at altitude. If bearing friction and inertia can be made minimal, a mechanical anemometer might give an acceptable measurement. Devices such as hot wires, vortex generators, spinning pressure probes, and sonic devices would all require considerable development for measuring winds at the top of a balloon. Therefore, for experimental flights to date, we have confined ourselves to observing motion of uninflated main balloon material, the fluttering motion of streamers attached to the tow line, and upper balloon motion, including both oscillation and rotation.

In this overall instrumentation we feel that we are developing a powerful tool for analysis of balloon structures during flight; the useful information already obtained encourages us to carry out more refined and more extensive experiments in the future.

LIST OF FIGURES

REFERENCE

Ney, E. P., R. W. Maas and W. F. Huch, 1961: The measurement of atmospheric temperature. J. Meteorol. 18(1), 60-80.